Zinc(II) ion mediates tamoxifen-induced autophagy and cell death in MCF-7 breast cancer cell line

Jung Jin Hwang · Ha Na Kim · Jean Kim · Dong-Hyung Cho · Mi Joung Kim · Yong-Sook Kim · Yunha Kim · Sung-Jin Park · Jae-Young Koh

Abstract Treatment of MCF-7 cells with tamoxifen induced vacuole formation and cell death. Levels of the autophagy marker, microtubule-associated protein light chain 3 (LC3)-II also increased, and GFP-LC3 accumulated in and around vacuoles in MCF-7 cells exposed to tamoxifen, indicating that autophagy is involved in tamoxifen-induced changes. Live-cell confocal microscopy with FluoZin-3 staining and transmission electron microscopy with autometallographic staining revealed that labile zinc(II) ion (Zn^{2+}) accumulated in most acidic LC3(+) autophagic vacuoles (AVs). Chelation of Zn^{2+} with N,N,N',N'-tetrakis (2-pyridylmethyl) ethylenediamine (TPEN) blocked the increase in phospho-Erk and LC3-II levels, and attenuated AV formation and cell death. Conversely, the addition of $ZnCl_2$ markedly potentiated tamoxifen-induced extracellular signal-regulated kinase (Erk) activation, autophagy and cell death, indicating that Zn^{2+} has an important role in these events. Tamoxifen-induced death was accompanied by increased oxidative stress and lysosomal membrane permeabilization (LMP) represented as release of lysosomal cathepsins into cytosol. Treatment with the antioxidant N-acetyl-L-cysteine (NAC) blunted the increase in Zn^{2+} levels and reduced LC3-II conversion, cathepsin D release and cell death induced by tamoxifen. And cathepsin inhibitors attenuated cell death, indicating that LMP contributes to tamoxifen-induced cell death. Moreover, TPEN blocked tamoxifen-induced cathepsin D release and increase in oxidative stress. The present results indicate that Zn^{2+} contributes to tamoxifen-induced autophagic cell death via increase in oxidative stress and induction of LMP.

Keywords Cathepsin · Extracellular signal-regulated kinase · Lysosome · Lysosomal membrane permeabilization ·

J. J. Hwang · D.-H. Cho · M. J. Kim · Y.-S. Kim · Y. Kim · S.-J. Park
Institute for Innovative Cancer Research, College of Medicine, University of Ulsan, Asan Medical Center, Seoul 138-736, Korea

H. N. Kim · J. Kim · J.-Y. Koh
Neural Injury Research Lab, Asan Institute for Life Science, College of Medicine, University of Ulsan, Asan Medical Center, Seoul 138-736, Korea

J.-Y. Koh (✉)
Department of Neurology, College of Medicine, University of Ulsan, 388-1 Poongnap-Dong Songpa-Gu, Seoul 138-736, Korea
e-mail: jkko@amc.seoul.kr

Present Address:
S.-J. Park
Laboratory of Bioimaging Probe Development, Singapore Bioimaging Consortium, Agency for Science, Technology and Research (A*STAR), Singapore 138667, Republic of Singapore

Microtuble-associated protein light chain 3 ·
Oxidative stress

Abbreviations

3-MA	3-methyladenine
AMG	Autometallography
ATG	Autophagy-related gene
AV	Autophagic vacuole
ER	Estrogen receptor
Erk	Extracellular signal-regulated kinase
Lamp-2	Lysosomal-associated membrane protein-2
LC3-II	Microtuble-associated protein light chain 3-II
LDH	Lactate dehydrogenase
LMP	Lysosomal membrane permeabilization
MT	Metallothionein
NAC	N-acetyl-L-cysteine
ROI	Region of interest
ROS	Reactive oxygen species
SERM	Selective estrogen receptor modulator
TPEN	N,N,N',N'-tetrakis (2-pyridylmethyl) ethylenediamine

Introduction

Tamoxifen is a nonsteroidal selective estrogen receptor modulator (SERM) commonly used in treatment of breast cancers as an antagonist (Jensen and Jordan 2003; Vijayanathan et al. 2006). Tamoxifen inhibits proliferation in estrogen receptor (ER)-positive breast cancer cells via competition with estradiol to bind to ER and modulation of gene expression (Watts et al. 1994). Besides ER-dependent transcriptional modulation, tamoxifen induces cell death in ER-negative cells independent to genomic regulation. It was reported that tamoxifen-induced cell death was autophagic cell death (Bursch et al. 1996) and mediated by reactive oxygen species generation and Erk activation (Bursch et al. 1996; Kallio et al. 2005; Zheng et al. 2007). However, the precise mechanism of tamoxifen-induced autophagic cell death has not been elucidated.

Autophagy (macroautophagy) is a major mechanism of self-degradation in cells. Autophagy starts with the formation of double-membraned autophagosomes around misfolded proteins and damaged organelles. Autophagosomes eventually fuse with lysosomes to form autolysosomes, which contain lysosomal acidic hydrolases that degrade the contents of the autophagosomes (Levine and Kroemer 2008; Mizushima et al. 2008; Nixon 2006). Autophagosomes and autolysosomes are also collectively called autophagic vacuoles (AVs). Although autophagy may have evolved as a defensive response to starvation in single-cell organisms, it has other diverse functions in multi-cellular organisms. For instance, chronic inhibition of autophagy may cause accumulation of toxic proteins and induce neurodegeneration (Levine and Kroemer 2008; Mizushima et al. 2008; Nixon 2006). Deficits in autophagy have also been implicated in the development of several forms of cancer, including breast cancer (Liang et al. 1999, 2001). Hence, understanding the process of autophagy may provide insights into the pathogenic mechanisms underlying various human diseases.

Although autophagy is essential for normal cellular functions, it also has a role in cell death under certain circumstances. Autophagic cell death or cell death with autophagy have been implicated in ischemic brain injury, heart and liver disease, and myopathies (Matsui et al. 2007; Mizushima et al. 2008; Uchiyama et al. 2008). While deficits in autophagy may induce cancer (Liang et al. 1999), several chemotherapeutic agents act by evoking autophagic cell death. For example, tamoxifen, causes AV formation and autophagic cell death in breast cancer cells (Bursch et al. 1996). Other examples include histone deacetylase inhibitors in chondrosarcoma cell lines (Yamamoto et al. 2008), rapamycin in malignant glioma (Takeuchi et al. 2005) and resveratrol in colon cancer cells (Ellington et al. 2005). The mechanism underlying autophagic cell death remains unclear, but lysosomal derangements, such as accumulation of lysosomes and lysosomal membrane permeabilization (LMP), are thought to be involved. Consistent with this idea, the accumulation of cathepsin D is reported to be linked to autophagy induction in osteoblastoma cells treated with doxorubicin (Zheng et al. 2008). Other mechanisms activated in autophagic cell death include reactive oxygen species (ROS) generation by NADPH oxidase (Chen et al. 2008; Scherz-Shouval et al. 2007), downregulation of the antiapoptotic proteins Bcl-X$_L$ and Bcl-2 (Feng et al. 2007; Pattingre et al. 2005), and activation of Erk and Jnk MAP kinases (Cheng et al. 2008).

Recently, we reported that oxidative injury induces LMP in hippocampal neurons (Hwang et al. 2008),

and further showed that: (1) labile Zn^{2+} accumulates in lysosomes prior to LMP by oxidative stress; (2) isolated lysosomes undergo LMP upon treatment with Zn^{2+}; and (3) chelation of Zn^{2+} markedly reduces LMP and neuronal cell death. Thus, endogenous Zn^{2+} may have a role in LMP-associated cell death. Since oxidative stress induces not only Zn^{2+}-mediated LMP but also autophagy, we hypothesized that labile Zn^{2+} may begin to accumulate in AVs before they fuse with lysosomes.

To investigate the role of Zn^{2+} in autophagy, we used the MCF-7 breast cancer cell line, in which tamoxifen-induced autophagic cell death has been well characterized. Thus, using tamoxifen-treated MCF-7 cells as a model system, we examined whether labile Zn^{2+} accumulates in AVs and, if so, whether labile Zn^{2+} has a role in early AV formation and in LMP and cell death.

Materials and methods

Cell culture and drug treatment

MCF-7 and SKBr-3 cells were cultured in RPMI 1640 containing 10% fetal bovine serum (FBS) and penicillin/streptomycin (Invitrogen, Carlsbad, CA, USA). Cells were treated with tamoxifen (Sigma, St. Louis, MO, USA) in serum-free RPMI 1640 medium for the indicated times. Depending on the experimental paradigm employed (see text for details), cells were pretreated for 30 min with $ZnCl_2$, *N,N,N′,N′*-tetrakis (2-pyridylmethyl) ethylenediamine (TPEN), 3-methyladenine (3-MA), rapamycin (Sigma), U0126 (Alexis, Lausen, Switzerland), PD98059 or *N*-acetyl-L-cysteine (Calbiochem, Darmstadt, Germany) prior to exposure to tamoxifen.

Live-cell confocal microscopy

Cells were stained with the fluorescent dyes, FluoZin-3-AM (5 μM), LysoTracker Red DND-99 (75 nM), LysoTracker Green DND-26 (75 nM) or MitoTracker Red CM-H_2-XRos (0.5 μM) (Invitrogen), in serum-free RPMI for 5–30 min in a humidified CO_2 incubator, and then transferred to Hank's balanced salt solution (HBSS). Live-cell images were acquired using an Ultra View Confocal Cell Imaging System

(PerkinElmer, Waltham, MA, USA) with an ECLIPSE TE2000 microscope (Nikon, Tokyo, Japan). All experiments were repeated at least three times. Analysis for colocalization was performed using the Ultra View software.

Fluorescent measurement for intracellular Zn^{2+}

Intracellular Zn^{2+} concentrations were determined with FluoZin-3-AM (Li and Maret 2009). In brief, 1×10^6 MCF-7 cells were treated with 17 μM tamoxifen in the presence or absence of 500 nM TPEN for 1 h, dissociated with 0.25% trypsin and washed with Dulbecco's phosphate-buffered saline (DPBS) without Ca^{2+} and Mg^{2+} (Invitrogen) three times. The cells were incubated with 0.3 μM Fluo-Zin-3 AM for 30 min at 37°C and washed with DPBS without Ca^{2+} and Mg^{2+} three times to remove any residual fluorescent dye. Fluorescence was measured with Spectramax Gemini XS (Molecular devices, Sunnyvale, CA, USA) at 25°C (excitation: 485 nm and emission: 538 nm). The same numbers of cells were incubated with 50 μM TPEN or with 100 μM pyrithione plus 250 μM $ZnSO_4$ for 10 min to measure background fluorescence of the dye (F_{min}) or maximum fluorescence (F_{max}), respectively. The concentrations of Zn^{2+} were calculated using the following equation (Li and Maret 2009):

$$\left[Zn^{2+}\right] = K_D(F - F_{min})/(F_{max} - F)(K_D = 8.9\,nM).$$

Transfection of MCF-7 cells with GFP-LC3 or RFP-LC3 and establishment of stable transformants

A defining feature of autophagosomes is the presence of the integral membrane protein LC3-II in AVs, which is derived by proteolytic cleavage of LC3 and by conjunction with the lipid phosphatidylethanolamine. When LC3-II is transfected into cells as a fluorescent fusion protein, LC3-II acts as an autophagosome marker that is invaluable in live-cell studies for morphological aspects of autophagy (Bampton et al. 2005; Kabeya et al. 2000). MCF-7 cells were transfected with pGFP-LC3 or pRFP-LC3 using Lipofectamine 2000 (Invitrogen) according to the manufacturer's instructions. After 1 day, the transfected cells were transferred to the selection

medium containing 2 mg/ml G418 until GFP-LC3- or RFP-LC3-expressing cell lines were established.

Quantification of cell death

Cell death was quantitatively assessed by measuring lactate dehydrogenase (LDH) activity released into the culture medium from damaged cells, as described previously (Koh and Choi 1987). Each LDH value was scaled to the mean value of cells exposed to 50 μM tamoxifen (100%) after subtracting the mean value of sham-washed control cells (0%).

Western blot analysis

For Western blot analysis, cells were rinsed with PBS and suspended in lysis buffer containing 20 mM Tris–Cl (pH 7.4), 150 mM NaCl, 1% Nonidet P-40, 0.5% sodium deoxycholate, 0.1% sodium dodecyl sulfate, and protease inhibitor cocktail (Roche, Indianapolis, IN, USA). The lysates were microcentrifuged at $12,000 \times g$ for 5 min and the supernatants were retained. Equal amounts of proteins were separated by sodium dodecyl sulfate-polyacrylamide gel electrophoresis (SDS-PAGE) and then transferred to polyvinylidene difluoride (PVDF) membranes (Millipore, Billerica, MA, USA). After blocking with 3% non-fat dry milk for 1 h, the membranes were incubated overnight at 4°C with primary antibodies against LC3 (Novus, Littleton, CO, USA), autophagy-related gene (ATG) 6 (also known as Beclin-1), phospho-Erk, Erk (Cell signaling, Beverly, MA, USA) or β-actin (Sigma), and then incubated with the appropriate horseradish peroxidase-conjugated secondary antibody (Pierce, Rockford, IL, USA). The Immobilon Western ECL solution (Millipore) and Kodak Image Station 4000MM (Kodak) were used to visualize the immunoreactive bands. Band intensities were analyzed by densitometry to quantify protein expression (Kodak Molecular Imaging software). The relative expression levels are presented as the ratio of LC3 II band density to the corresponding density of β-actin bands.

Western blot analysis of cathepsins released from lysosome into cytosol

As described previously (Hwang et al. 2008), we extracted cytosolic proteins using digitonin (Sigma)

which disrupts plasma membrane leaving cellular organelle in the cell pellets (Plutner et al. 1992). In brief, cytosolic proteins were extracted with extraction buffer (250 mM sucrose, 20 mM HEPES, 10 mM KCl, 1.5 mM $MgCl_2$, 1 mM EDTA, and 1 mM EGTA) containing 25 μg/ml digitonin by rocking (100 rpm) on ice for 15 min. Protein in the cytosolic extracts was precipitated with 10% trichloroacetic acid, washed with methanol, and lysed with lysis buffer (20 mM Tris–Cl pH 7.4, 150 mM NaCl, 1 mM EDTA, 1 mM EGTA, 1% Triton X-100, 2.5 mM sodium pyrophosphate, 1 μM Na_3VO_4, 1 μg/ml Leupeptin, and 1 mM phenylmethylsulfonyl fluoride). Equal amounts of proteins were separated by SDS-PAGE and analyzed by western blotting using antibodies against cathepsin D (Santa Cruz, Santa Cruz, CA, USA), and tubulin (Cell signaling), as described above.

Immunocytochemistry

Cells were fixed with 4% paraformaldehyde (Sigma) and incubated for 30 min at room temperature in blocking solution containing 1% bovine serum albumin (Sigma) and 0.2% Triton X-100. The cells were then incubated overnight at 4°C with anti-ATG6 (Cell signaling), anti-Cathepsin B and D (Santa Cruz Biotechnology), human-specific anti-lysosomal-associated membrane protein-2 (Lamp-2, Developmental Studies Hybridoma Bank, Iowa City, IA, USA), and anti-HNE antibodies (Alpha Diagnostic, San Antonio, TX, USA) in PBS containing 0.5% sodium azide. Thereafter, samples were incubated at room temperature for 1 h with Alexa Fluor-conjugated secondary antibodies (Invitrogen). Three-dimensional images of stained cells were obtained by z-series analysis using a confocal microscope (TCS-SP2; Leica, Nussloch, Germany). Colocalization analysis was performed using Image J Mander's coefficients.

Electron microscopy of autometallography (AMG)-stained MCF-7 cell

For AMG staining, MCF-7 cells exposed to 17 μM tamoxifen for the indicated times were incubated with 15 mg/ml selenium for 15 min at 37°C in a humidified CO_2 incubator, and then rinsed with RPMI media. The cells were fixed in 3% glutaraldehyde in 0.1 M phosphate buffer (PB) for 5 min at

room temperature, and then at 4°C for 30 min. After washing three times with PB and briefly rinsing in distilled water, the samples were submerged in AMG kit reagent (HQ silver enhancement, Nanoprobes, Yaphank, NY, USA) for 90 s at room temperature. The reaction was stopped by washing the samples with 0.1 M PB. Cells were post fixed in 1% OsO4 in PB for 20 min, washed again with 0.1 M PB, and then dehydrated in a graded series of ethanol. During the dehydration procedure, cells were stained with 1% uranylacetate in 70% ethanol for 10 min, infiltrated in a graded series of Epon 812 and embedded in Epon 812. After the embedded block had been cured at 60°C for 3 days, ultrathin sections (70–90 nm thick, Reichert-Jung, Germany) were collected on 200 mesh grids coated with 2% collodion and examined using a transmission electron microscope (JEOL model 1200EX, Tokyo, Japan).

ROS staining

Tamoxifen-treated cells were incubated with 10 μM $H_2DFF-DA$ for 30 min in serum-free RPMI, washed with serum-free RPMI, and then observed under an inverted fluorescence microscope (IX70, Olympus, Tokyo, Japan). Fluorescent intensity was analyzed with ROI manager of Image J software.

siRNA transfections

MCF-7 cells were transfected with 250 nM SMART-pool siRNA targeting ATG6 or control non-targeting siRNA pool (Dharmacon, Lafayette, CO, USA) using Lipofectamine 2000, cultured for 2 days, and then treated with 17 μM tamoxifen for the indicated times.

Results

Tamoxifen induces vacuolar changes and cell death in MCF-7 cells

At 10 μM, tamoxifen was not toxic to MCF-7 cells after exposure for 24 h, but induced approximately 70% cell death at 20 μM and near-complete cell death at concentrations of 30–50 μM (Fig. 1a). These results yielded an estimated median lethal concentration (LC_{50}) value for tamoxifen of approximately 17 μM. The time course of LDH release showed that higher doses of tamoxifen induced more rapid cell death; at 30 μM, tamoxifen induced total LDH release after 5 h (Fig. 1b). In subsequent experiments, we used tamoxifen at its LC_{50} of 17 μM unless otherwise indicated.

Tamoxifen-induced changes in MCF-7 cell morphology started within 1 h, beginning with the

Fig. 1 Tamoxifen induces vacuolar changes and cell death in MCF-7 cells. **a** Data represent LDH release (mean + SD, $n = 3$) 24 h after exposure to the indicated concentrations of tamoxifen. **b** LDH release ($n = 3$) at the indicated times after continuous exposure to 17, 20 or 30 μM tamoxifen. **c** Phase-contrast photomicrographs of sham-washed control MCF-7 cells (CTL) or cells treated for 4 or 12 h with 17 μM tamoxifen (TAM). Note prominent vacuoles. Scale bar, 100 μm
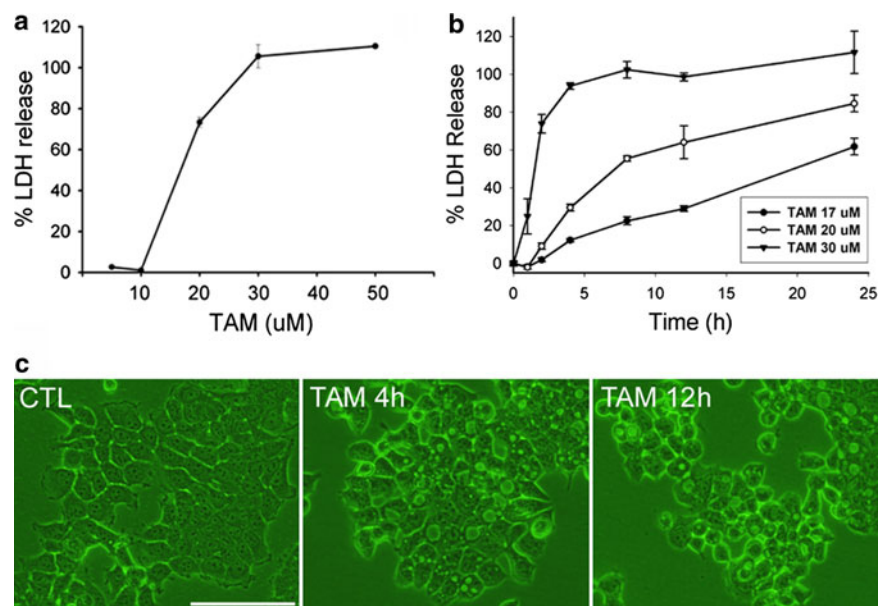
appearance of small, dark vacuoles in the cytosol of a small number of cells (not shown). Cytosolic vacuoles were evident in most MCF-7 cells after 4 h of exposure to 17 μM tamoxifen and became highly conspicuous; the number of vacuoles continued to increase until the 12-h time point (Fig. 1c). By 24 h, cells had rounded up and detached from the dish (not shown).

Tamoxifen-induced AV formation and autophagic cell death

To determine if autophagy is activated by tamoxifen, we harvested MCF-7 cells at the indicated times after a sham washing (control) or exposure to 17 μM tamoxifen. Western blot analysis of LC3-I and LC3-II revealed that tamoxifen treatment increased the level of LC3-II that was evident after 30 min and persisted for 8 h (Fig. 2a, b). To observe AV formation, we made MCF-7 cells expressing pGFP-LC3 permanently (GFP-MCF-7 cells), and analyzed

cells for GFP fluorescence using live-cell confocal microscopy. The number of LC3(+) vacuoles continued to increase from 60 to 90 min after initiation of tamoxifen treatment (Fig. 2c and movie 1 in supplemental material). LC3 fluorescence (arrows) was detected in a ring-shaped pattern, consistent with localization to the AV membrane. Immunocytochemistry for ATG6 (Beclin 1) showed that ATG6 was localized mainly to LC3(+) puncta in tamoxifen-treated cells, whereas in controls both ATG6 and LC3 showed more diffuse pattern of staining (Fig. 2d).

To confirm that the pattern of LC3 distribution reflected an autophagic process, we inhibited class III phosphoinositide 3-kinase (PI3K), which is essential for activation of autophagy, with the widely used PI3K inhibitor 3-methyladenine (3-MA) (Fig. 2e). Tamoxifen increased the number of LC3(+) AVs in GFP-MCF-7 cells. This increase in the formation of LC3(+) AVs was blocked by pretreatment with 1 mM 3-MA; this also blocked tamoxifen-induced MCF-7 cell death, indicating that AV formation is a
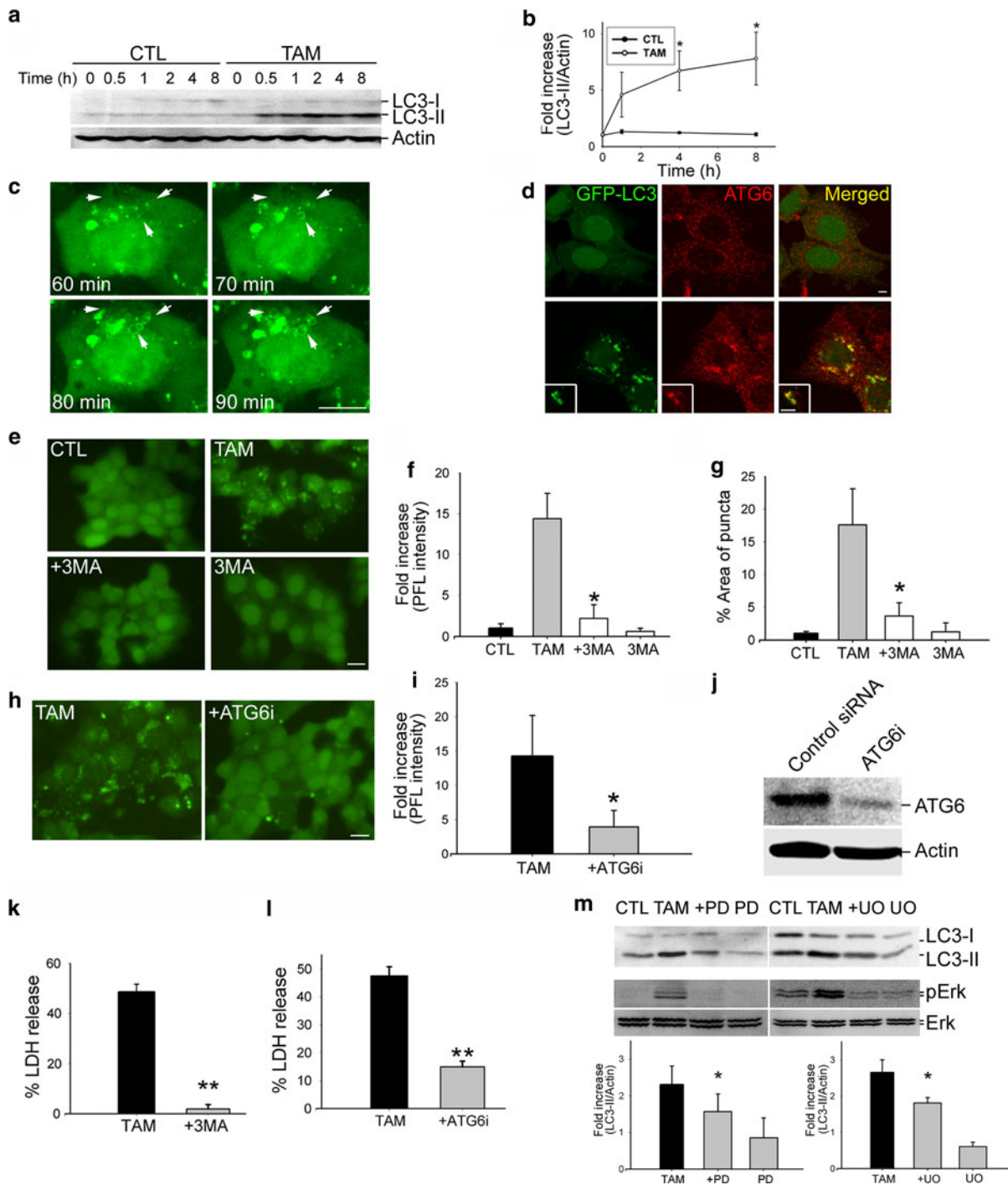
necessary step in tamoxifen-induced cell death (Fig. 2k). As shown in Fig. 2f and g, pretreatment with 3-MA blocked tamoxifen-induced increase in fluorescent intensity of puncta per cell as well as

percent area occupied by AVs. Consistent with this observation, silencing ATG6 gene using siRNA (Fig. 2j) also decreased AVs (Fig. 2h, i) and cell death (Fig. 2l) induced by tamoxifen, further

supporting that tamoxifen-induced vacuoles and cell death are largely autophagic in nature.

Tamoxifen activates Erk, and the Mek inhibitor, PD98059, attenuates cell death by tamoxifen (Zheng et al. 2007) and autophagy by TNFα (Cheng et al. 2008), so it is possible that activation Erk contributes to conversion of LC3-I to LC3-II induced by tamoxifen. Pretreatment of MCF-7 cells with Mek inhibitors (20 μM PD98059 or 10 μM U0126) attenuated the conversion of LC3-I to LC3-II (Fig. 2m) induced by tamoxifen.

Zinc(II) ions in tamoxifen-induced AVs

To determine if Zn^{2+} accumulates in AVs, we loaded MCF-7 cells with the zinc-specific fluorescent dye FluoZin-3, and then treated cells with tamoxifen. An analysis of cells by live-cell confocal microscopy revealed rapid accumulation of Zn^{2+} in vacuoles and cytosol (Fig. 3a and movie 2 and 3 in supplemental material). As shown in Fig. 3b, intracellular Zn^{2+} concentrations are 0.066 nM in control MCF-7 cells and 0.286 nM in tamoxifen-treated cells. TPEN
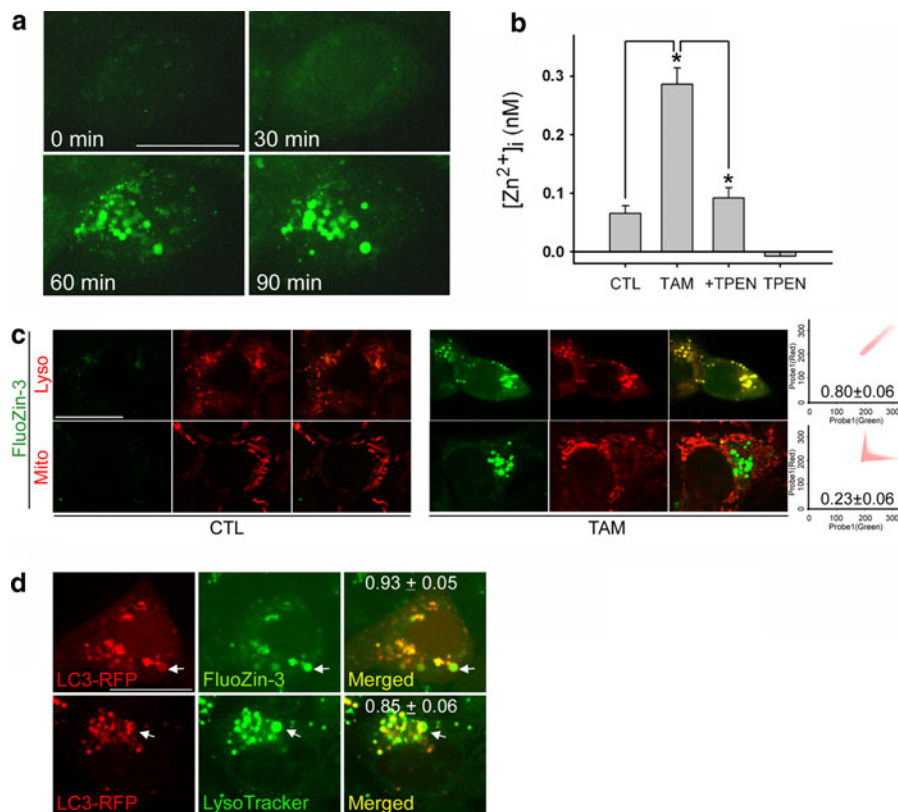
Fig. 3 Zinc(II) ions in tamoxifen-induced AVs. a Live-cell confocal microscopic images of MCF-7 cells stained with FluoZin-3 at the indicated times (minutes) after the addition of 17 μM tamoxifen. Images are from a z-series (35 z-section images, 1 μm thick). Scale bar, 10 μm. b Intracellular concentration of Zn^{2+} ([Zn^{2+}]$_i$) in MCF-7 cells treated with 17 μM tamoxifen with or without 500 nM TPEN for 1 h. [Zn^{2+}]$_i$ was measured using FluoZin-3-AM as described in the Materials and methods. (mean + SEM, $n = 4$–6; paired t-test, $*P < 0.05$). c MCF-7 cells were double-stained with FluoZin-3 and LysoTracker-Red (Lyso) or MitoTracker-Red (Mito). In control cells (CTL), the levels of Zn^{2+} were low in the cytosol, lysosomes and mitochondria. In contrast, the levels of Zn^{2+} increased in the cytosol and lysosomes, but not in

mitochondria, of cells that developed vacuoles 90 min after treatment with 17 μM tamoxifen (TAM). Images are from a single z-section. Scale bar, 10 μm. Each correlation plot of tamoxifen-treated cells is derived from an image shown using the Ultra View software. The mean correlation coefficient (c) ±SD of 5 images are shown on the plots (right graphs). d RFP-LC3-transfected cells were treated with 17 μM tamoxifen for 90 min and stained with FluoZin-3 (upper panel) or Lyso-Tracker-Green (lower panel), respectively. There was substantial overlap between Zn^{2+}, LC3 and lysosome staining. Note the ring-pattern of RFP-LC3 fluorescence that surrounds zinc or LysoTracker fluorescence (Arrows). Images are from a single z-section. Each mean correlation coefficient (c) ±SD of 10 cells is shown in each merged image. Scale bar, 10 μm

reduced the increase in intracellular Zn^{2+} by tamoxifen to the basal level (0.092 nM).

To determine whether zinc-containing vacuoles overlapped with lysosomes in these cells, we double-stained tamoxifen-treated and control MCF-7 cells with FluoZin-3 and LysoTracker or MitoTracker. Live-cell confocal microscopy revealed that most of the zinc(+) vacuoles co-stained with LysoTracker (the correlation coefficient (c) = 0.80 ± 0.06) but not with MitoTracker (c = 0.23 ± 0.06) (Fig. 3c). Additional co-localization studies using RFP-LC3-transfected cells showed that almost all zinc(+) vacuoles were LC3(+) AVs (c = 0.93 ± 0.05), which were also co-stained with LysoTracker (c = 0.85 ± 0.06) (Fig. 3d). To obtain more direct evidence for Zn^{2+} in AVs, we stained MCF-7 cells with zinc AMG and observed them by transmission electron microscopy. AMG staining revealed that, whereas no AMG(+) vacuoles were observed in control cells (Fig. 4a), double- or multi-membraned vacuoles containing AMG grains were present in cells treated with tamoxifen for 30 min, indicating that labile Zn^{2+} is indeed present in AVs (Fig. 4b). After a 2-h exposure to tamoxifen, single-membraned autolysosomes containing AMG grains were observed (Fig. 4c).

The role of zinc in tamoxifen-induced autophagy and cell death

The fact that Zn^{2+} accumulates in AVs induced by tamoxifen indicates that Zn^{2+} may have a role in AV formation. To test this, we examined the effects of Zn^{2+} or a zinc chelator, TPEN, on tamoxifen-induced AV formation. Tamoxifen induced conspicuous vacuole formation, and the addition of 50 μM $ZnCl_2$, which alone did not induce any vacuoles (not shown), further increased vacuole formation (Fig. 5a). Conversely, the addition of 500 nM TPEN reduced tamoxifen-induced AV formation (Fig. 5a). Consistent with these findings, Western blot analyses revealed that the levels of LC3-II were augmented by the addition of 50 μM Zn^{2+} (Fig. 5b) but reduced by the addition of 500 nM TPEN (Fig. 5c). Zn^{2+}-dependent increase in LC3-II was also induced by low dose (5 μM) of tamoxifen in MCF-7 cells (Fig. 5d). Moreover, augmentation of LC3-II by tamoxifen required Zn^{2+} not only in ER-positive
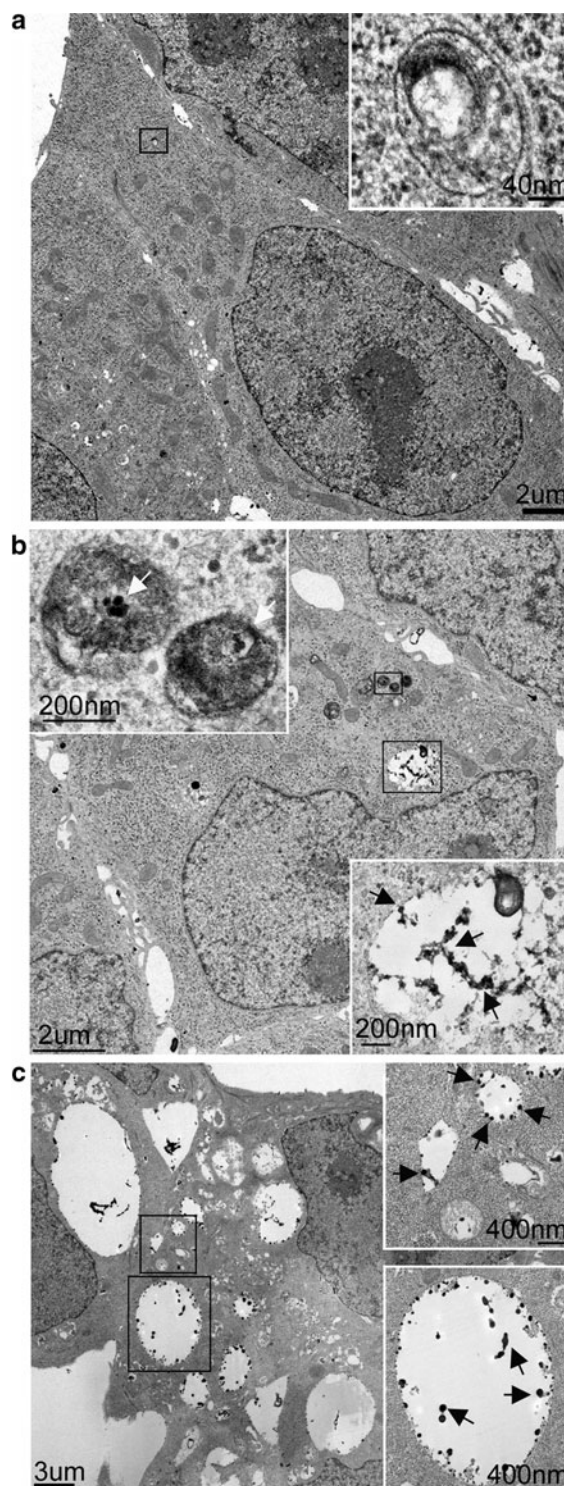

Fig. 4 Zinc(II) ions stained with AMG in AVs. **a–c**. Transmission electron micrographs of AMG-stained MCF-7 control cells (**a**) or cells treated with 17 μM tamoxifen for 30 min (**b**) or 2 h (**c**)

Figure showing panels a–i with Western blots and bar graphs.

a CTL | TAM | +Zn | +TPEN

b
TAM − + + −
Zn   − − + +
LC3-I, LC3-II, Actin

Bar graph: Fold increase (LC3-II/Actin); CTL, TAM (#), +Zn (*), Zn (#)

c
TAM   − + + −
TPEN − − + +
LC3-I, LC3-II, Actin

Bar graph: Fold increase (LC3-II/Actin); CTL, TAM (#), +TPEN (*), TPEN

d
TAM$_{low}$ − + + −
TPEN   − − + +
LC3-I, LC3-II, Actin

e
TAM   − + + −
TPEN − − + +
SKBr-3
LC3-I, LC3-II, Actin

f
TAM − + + −
Zn   − − + +
pErk, Erk

Bar graph: Fold increase (pErk/Erk); TAM, +Zn (*), Zn (#)

g Bar graph: % LDH release; TAM, +Zn (**), Zn

h
TAM   − + + + − −
TPEN − − 50 500 50 500
pErk, Erk

Bar graph: Fold increase (pErk/Erk); TAM, +TPEN (*), TPEN

i Bar graph: % LDH release; TAM, +TPEN (*), TPEN

MCF-7 cells but also ER-negative SKBr-3 cells (Fig. 5e). Activation of Erk contributes to autophagy induced by tamoxifen (Fig. 2m) and Zn^{2+} activates Erk (Park and Koh 1999) and autophagy (Fig. 5a–c), so it is possible that the increase in intracellular Zn^{2+} induced by tamoxifen contributes to by Erk activation. Zn^{2+} potentiated tamoxifen-induced Erk phosphorylation and TPEN inhibited this change (Fig. 5f, h). In addition, the same pattern was observed for cell death. Although 15 μM tamoxifen induced a low degree of cell death, exposure of MCF-7 cells to a non-toxic dose of Zn^{2+} (20 μM) markedly potentiated tamoxifen-induced

cell death (Fig. 5g). Conversely, the addition of 40 nM TPEN significantly attenuated tamoxifen-induced cell death (Fig. 5i). These results indicate that the tamoxifen-induced increase in intracellular Zn^{2+} mediates autophagic cell death in MCF-7 cells.

Evidence for tamoxifen-induced lysosomal membrane permeabilization

In autophagy, AVs fuse with lysosomes to form autophagolysosomes, also called autolysosomes. It is possible that autophagic cell death involves membrane

◄ **Fig. 5** The role of zinc(II) ions in tamoxifen-induced autophagy and cell death. **a** Phase-contrast photomicrographs of MCF-7 cells after a 4-h exposure to 17 μM tamoxifen (TAM), tamoxifen plus 50 μM $ZnCl_2$ (+Zn) or tamoxifen plus 500 nM TPEN (+TPEN). Whereas the addition of $ZnCl_2$ markedly increased the number of AVs induced by tamoxifen, the addition of TPEN attenuated AV formation. Scale bar, 100 μm. **b** Western blot analysis of LC3-I and LC3-II from MCF-7 cells treated with 17 μM tamoxifen or tamoxifen plus 50 μM $ZnCl_2$ for 1 h. The addition of $ZnCl_2$ increased the level of tamoxifen-induced LC3-II and $ZnCl_2$ alone converted LC3-I to LC3-II. The *bar graph* represents densitometric measurements of the LC3-II bands expressed relative to the corresponding β-actin bands and normalized to the LC3-II/β-actin ratio in controls (mean + SD, $n = 3$; paired t-test, *$P < 0.05$ compared to tamoxifen alone, #$P < 0.05$ compared to control). **c** Western blot analysis of LC3-I and LC3-II from MCF-7 cells treated with 17 μM tamoxifen or tamoxifen plus 500 nM TPEN for 1 h. The *bar graph* represents densitometric measurements of the LC3-II bands from cells treated with 17 μM tamoxifen or tamoxifen plus 500 nM TPEN expressed relative to the corresponding β-actin bands and normalized to the LC3-II/β-actin ratio in controls (mean + SD, $n = 4$; paired t-test, *$P < 0.05$ compared to tamoxifen alone, #$P < 0.05$ compared to control). **d** Western blots analysis of LC3-I and LC3-II from MCF-7 cells treated with 5 μM tamoxifen (TAM$_{low}$) or tamoxifen plus 500 nM TPEN for 4 h. Low dose of tamoxifen increased LC3-II in a Zn^{2+}-dependent manner. **e** Western blot analysis of LC3-I and LC3-II from ER-negative SKBr-3 cells treated with 17 μM tamoxifen or tamoxifen plus 500 nM TPEN for 1 h. Tamoxifen increased LC3-II in ER-negative breast cancer cells and required Zn^{2+} for autophagy activation. **f** Western blot analysis of phospho-Erk (pErk) and Erk from cells treated with 17 μM tamoxifen or tamoxifen plus 50 μM $ZnCl_2$ for 1 h. The addition of Zn^{2+} increased tamoxifen-induced Erk phosphorylation. Exposure to tamoxifen or Zn^{2+} had no effect on the level of total cellular Erk. The *bar graph* represents densitometric measurements of the pErk bands from cells treated with 17 μM tamoxifen or tamoxifen plus 50 μM $ZnCl_2$ for 1 h expressed relative to the corresponding Erk bands and normalized to the pErk/Erk ratio in controls (mean + SD, $n = 3$–6; paired t-test, *$P < 0.05$ compared to tamoxifen alone, #$P < 0.05$ compared to control). **g** The *bar graph* denotes LDH release after a 24-h exposure to 15 μM tamoxifen (TAM) or tamoxifen plus 20 μM $ZnCl_2$ (+Zn) (mean + SD, $n = 3$; paired t-test, **$P < 0.01$ compared to tamoxifen alone). Treatment with 15 μM tamoxifen or 20 μM $ZnCl_2$ (Zn) did not induced LDH release. **h** Western blot analysis of phospho-Erk (pErk) and Erk from cells treated with 17 μM tamoxifen or tamoxifen plus 50 or 500 nM TPEN for 1 h. TPEN blocked tamoxifen-induced Erk phosphorylation. Exposure to tamoxifen or TPEN had no effect on the level of total cellular Erk. The *bar graph* represents densitometric measurements of the pErk bands from cells treated with 17 μM tamoxifen or tamoxifen plus 500 nM TPEN for 1 h expressed relative to the corresponding Erk bands (mean + SD, $n = 3$–6; paired t-test, *$P < 0.05$ compared to tamoxifen alone). **i** The *bar graph* denotes LDH release after a 24-h exposure to 17 μM tamoxifen (TAM) or tamoxifen plus 40 nM TPEN (+TPEN) (mean + SD, $n = 3$; paired t-test, *$P < 0.05$ compared to tamoxifen alone). Treatment with 40 nM TPEN (TPEN) did not induced LDH release

permeabilization of over-loaded autolysosomes, a process that may be equivalent to the lysosomal membrane permeabilization (LMP) described in many cases of cell death (Kroemer and Jaattela 2005). To assess changes in lysosomal morphology, we stained cells with an antibody against the lysosomal marker lysosomal-associated membrane protein-2 (Lamp-2). Tamoxifen treatment markedly increased the size of lysosomes but tended to reduce their number (Fig. 6a). As expected, addition of 500 nM TPEN completely blocked these tamoxifen-induced morphological changes (Fig. 6a). Consistent with an LMP process, cathepsin B and D immunoreactivity was increased in the cytosol of tamoxifen-treated cells, and this change was reversed by TPEN (Fig. 6b). We have previously shown that 4-hydroxynonenal (HNE) accumulation may contribute to LMP in hippocampal neurons under conditions of oxidative stress (Hwang et al. 2008). Consistent with these findings, we found that HNE immunoreactivity was markedly increased after exposure of MCF-7 cells to tamoxifen, an effect that was reversed by TPEN (Fig. 6c).

To confirm that LMP occurs in tamoxifen-induced autophagic cell death, we examined cytosolic levels of cathepsin D by Western blot analyses. Both intermediate and mature forms of cathepsin D were markedly increased in the cytosol 4 h after initiating tamoxifen treatment, in consistence with the release of cathepsin D from lysosomes (Fig. 6d, e). The addition of TPEN or the antioxidant *N*-acetyl-L-cysteine (NAC) blocked the tamoxifen-induced increase in cytosolic cathepsin D levels, indicating that changes in LMP require endogenous Zn^{2+} as well as oxidative stress. A cathepsin B inhibitor and a specific cathepsin D inhibitor (pepstatin A) attenuated tamoxifen-induced cell death, as did the antioxidant NAC (Fig. 6f). In addition, NADPH oxidase inhibitors (diphenyleneiodonium chloride (DPI) and apocynin) blocked cell death by tamoxifen,

Oxidative stress is required for LMP and autophagy

Because oxidative stress induces both lysosomal Zn^{2+} accumulation and LMP, we examined the effect of tamoxifen on oxidative stress in MCF-7 cells using H_2DFF fluorescence to estimate levels of oxidative stress (Fig. 7a, b). In contrast to sham-washed (control) cells, in which H_2DFF fluorescence
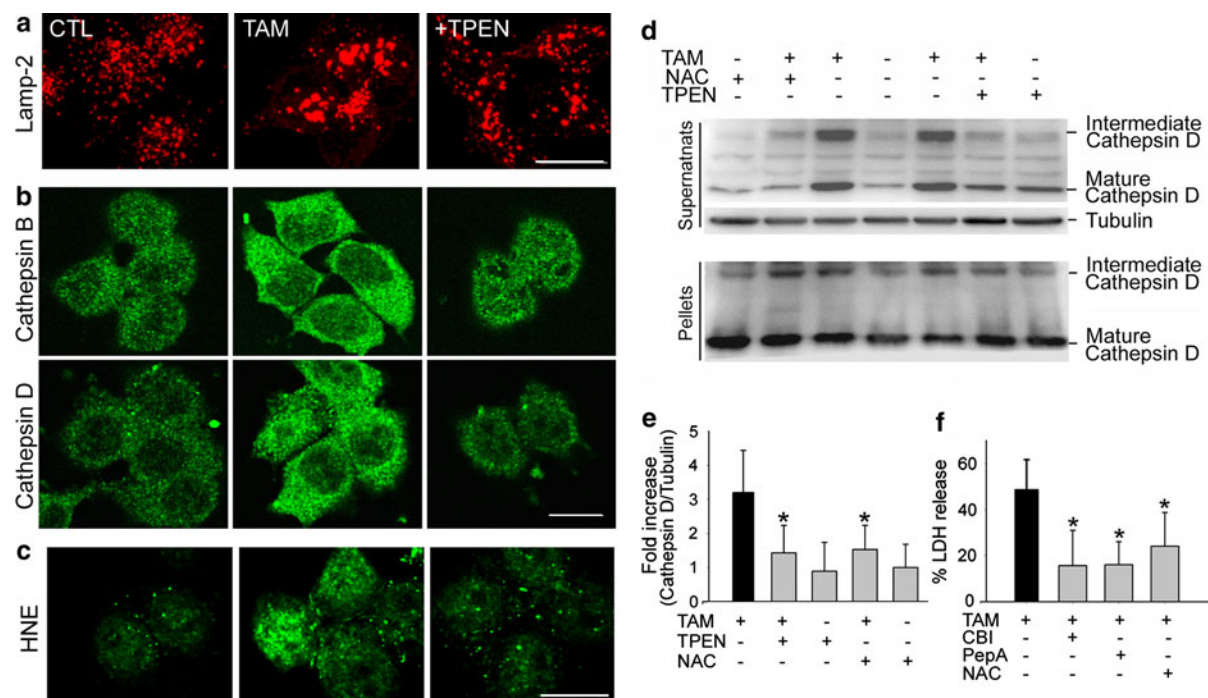
Fig. 6 Evidence for LMP in tamoxifen-treated cells. a Fluorescence confocal micrographs of MCF-7 cells stained with anti-Lamp-2 antibody. Treatment with 17 μM tamoxifen for 1 h (TAM) increased the size of lysosomes compared with sham-washed controls (CTL). The addition of 500 nM TPEN (+TPEN) blocked this effect of tamoxifen. Images are from a z-series (12-15 images, 1 μm thick). Scale bar, 10 μm. b Fluorescence confocal micrographs of MCF-7 cells stained with anti-cathepsin B and D antibodies. Tamoxifen treatment increased cathepsin B and D immunoreactivity in the cytosol compared with sham-washed controls. The addition of 500 nM TPEN blocked this effect of tamoxifen. Images are from a single z-section. Scale bar, 10 μm. c Fluorescence confocal micrographs of MCF-7 cells stained with anti-HNE adduct antibody. Tamoxifen treatment increased the level of HNE immunoreactivity compared with sham-washed controls. The addition of 500 nM TPEN blocked this effect of tamoxifen. Images are from

a z-series (12–15 images, 1 μm thick). Scale bar, 10 μm. d Western blot analysis of cathepsin D in cytosolic fractions (Supernatants) and pellets (membrane-enriched fraction) obtained from MCF-7 cells after a 4-h exposure to 17 μM tamoxifen (TAM) or tamoxifen plus 500 nM TPEN or 1 mM NAC. Tubulin was used as a loading control. The addition of TPEN or NAC blocked the tamoxifen-induced release of intermediate and mature cathepsin D into cytosol. e Data in the graph represent fold increases in the mature cathepsin D/tubulin density ratio of MCF-7 cell treated with 17 μM tamoxifen (TAM) or tamoxifen plus 500 nM TPEN or 1 mM NAC; cathepsin D/tubulin ratio in control was taken as 1 (mean + SD, $n = 4$–5; paired t-test, *$P < 0.05$ compared to control). f Bars denote LDH release after a 24-h exposure to 17 μM tamoxifen or tamoxifen plus 100 nM cathepsin B inhibitor (CBI), 10 μM pepstatin A (PepA) or 1 mM NAC (mean + SD, $n = 3$–7; paired t-test, *$P < 0.05$ compared to tamoxifen alone)

was negligible, fluorescence was high in MCF-7 cells treated with 17 μM tamoxifen for 4 h. This increase in fluorescence was completely blocked by the antioxidant 1 mM NAC. NAC also attenuated vacuole formation (phase-contrast images, Fig. 7a) and increased the level of LC3-II (Fig. 7c) induced by tamoxifen, thus confirming that ROS is also necessary for the initiation of autophagy by tamoxifen. Moreover, NAC abolished the tamoxifen-induced increase in Zn^{2+}, indicating that ROS accelerates tamoxifen-induced Zn^{2+} accumulation (Fig. 7d).

Conversely, addition of zinc chelator TPEN reduced the accumulation of ROS (Fig. 7b, e), indicating the existence of a positive feedback between Zn^{2+} accumulation and oxidative stress in tamoxifen-induced MCF-7 cell death.

Discussion

The main finding of the present study is that tamoxifen-induced AVs in MCF-7 breast cancer cells
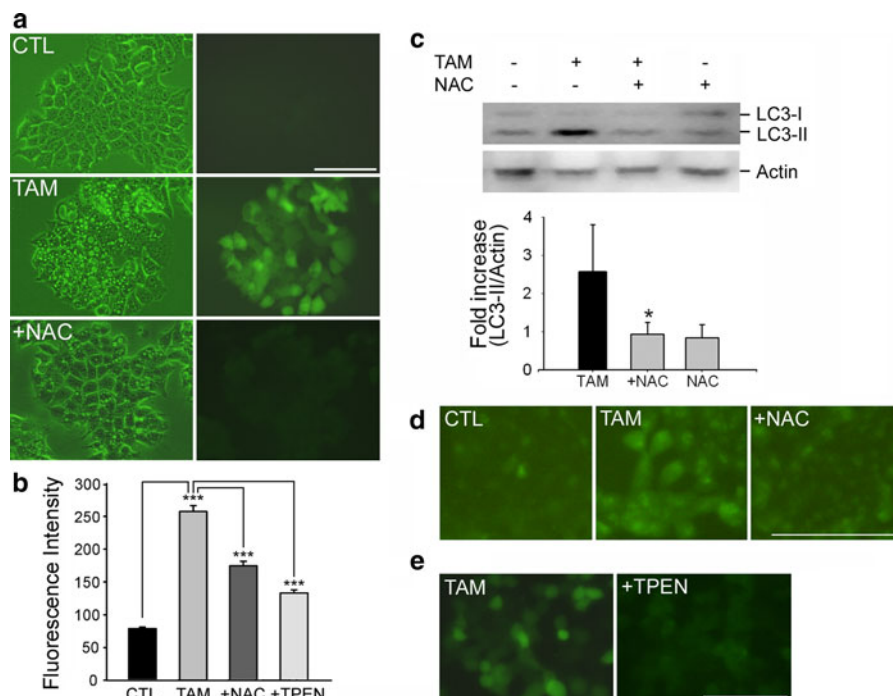
Fig. 7 Oxidative stress is required for LMP. **a** Phase-contrast (*left*) and H_2DFF fluorescence (*right*) micrographs of MCF-7 cells. *Upper:* Sham-washed control. *Middle:* After a 4-h exposure to 17 μM tamoxifen; tamoxifen markedly increased the level of ROS in MCF-7 cells. *Lower:* Addition of 5 mM NAC inhibited the rise in ROS levels and blocked AV formation induced by tamoxifen. Scale bar, 100 μm. **b** Fluorescent intensity of H_2DFF from the cell treated with 17 μM tamoxifen alone (TAM), tamoxifen plus 5 mM NAC (+NAC) or tamoxifen plus 500 nM TPEN (+TPEN). Data obtained from more than 40 cells in each picture were analyzed using Image J program (mean + SEM, $n = 3$, Student t-test, ***$P < 0.0001$). **c** Western blot analysis of LC3 from cells treated with 17 μM tamoxifen or tamoxifen plus 1 mM NAC for 4 h. NAC reversed the tamoxifen-induced increase in LC3-II levels. β-actin was used as a loading control. *Bars* represent densitometric measurements of the LC3-II bands from cells treated with 17 μM tamoxifen or tamoxifen plus NAC expressed relative to the corresponding β-actin bands (mean + SD, $n = 4$; paired t-test, *$P < 0.05$ compared to tamoxifen alone). **d** FluoZin-3 fluorescence micrographs of sham-washed (CTL) MCF-7 cells, or cells treated for 4 h treatment with 17 μM tamoxifen (TAM) or tamoxifen plus 1 mM NAC (+NAC). Addition of NAC attenuated the increase in Zn^{2+} signals induced by tamoxifen. Scale bar, 100 μm. **e** H_2DFF fluorescence micrographs of MCF-7 cells after a 4-h treatment with 17 μM tamoxifen (TAM) or tamoxifen plus 500 nM TPEN (+TPEN). Note that TPEN blocked the tamoxifen-induced increase in ROS. Scale bar, 100 μm

accumulate high levels of Zn^{2+}. In addition, intracellular zinc chelator TPEN blocked tamoxifen-induced autophagy, indicating the possible role of Zn^{2+} therein. Tamoxifen is a widely used antineoplastic agent. It is well known that tamoxifen induces growth arrest or various forms of cell death including apoptosis and autophagic cell death, depending on doses (Bursch et al. 1996). The tamoxifen concentration used in the present study (17 μM) was chosen because it induced excess autophagy accompanied by conspicuous cell death in 24 h. It is likely that with more prolonged exposure, toxic concentrations of tamoxifen are lower.

Tamoxifen is a selective estrogen receptor modulator primarily used against ER(+) breast cancer (Jensen and Jordan 2003; Vijayanathan et al. 2006). Although blockade of ER may be important for its anticancer effect in ER(+) cells, at doses approximately four fold to eight fold above those used for ER inhibition, tamoxifen shows therapeutic activity in ER(−) tumors, including glioma, melanoma, pancreatic carcinoma, lung cancer, and renal cell carcinoma (Gelmann 1997; Heerdt and Borgen 1999; Lee et al. 2000a). Our results showed that tamoxifen increased LC3-II conversion in both ER-positive MCF-7 and ER-negative SKBr-3 breast cancer cells (Fig. 5b, e),
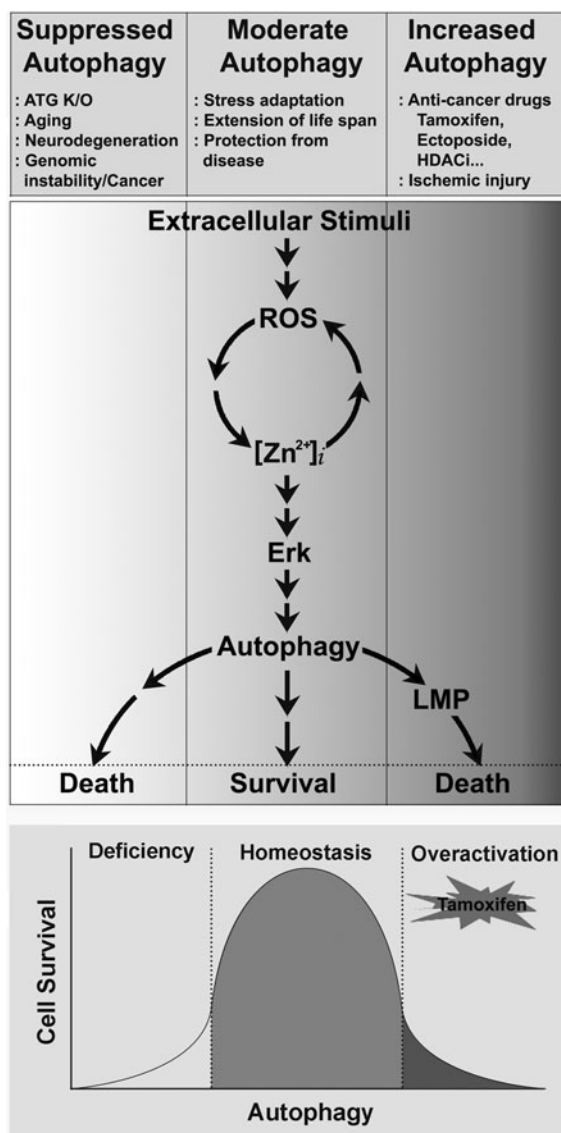
Fig. 8 A diagram for toxic mechanism of action by tamoxifen. Tamoxifen increases ROS production and intracellular Zn^{2+} levels in MCF-7 cells. Increases in intracellular ROS and Zn^{2+} resulted in activation of ERK and autophagy. Whereas adequate levels of autophagy may be beneficial for cell survival, excessive levels of autophagy such as induced by toxic levels of tamoxifen, may result in LMP and cell death. It can be the mechanism of other anticancer drugs, such as ectoposide or histone deacetylase inhibitor (HDACi) that are known to induce autophagic cell death. In contrast, too low levels of ROS production and labile Zn^{2+} may lead to diminished autophagy, which renders cells more vulnerable to various insults. It is in the cases of ATG knock out (ATG K/O) or aging, leading to neurodegeneration or cancer

indicating that tamoxifen-induced autophagy is independent to ER. Recently, tamoxifen has been shown to induce autophagy and autophagic cell death in breast and colon cancer cells (de Medina et al. 2009; Scarlatti et al. 2004) in an Erk-dependent manner (Zheng et al. 2007). Consistent with these reports, tamoxifen, at 17 μM, induces LC3-II conversion, AV formation and cell death in MCF-7 cells also in an Erk-dependent fashion. Since Zn^{2+} also activates Erk via inhibition of phosphatase (Haase and Maret 2003) or activation of receptor tyrosine kinase (Hwang et al. 2005), it is possible that tamoxifen activates Erk via an increase in the level of intracellular Zn^{2+}. The near complete blockade of cell by 3-MA, an inhibitor of autophagy, strongly suggests that tamoxifen-induced cell death is indeed autophagic in nature.

Since almost all zinc tightly binds to proteins, concentration of total zinc in mammalian cells is several hundred micromolar but the concentration of free Zn^{2+} is only picomolar (Li and Maret 2009). Regardless, free Zn^{2+} is increasingly recognized as a mediator of key intracellular signaling events, including cell death (Choi and Koh 1998; Frederickson et al. 2005). Yet despite this awareness and the keen research interest in autophagy on the part of investigators working in diverse fields of biology, the role of endogenous Zn^{2+} in autophagy has not been considered. Our results demonstrate a role for Zn^{2+} in tamoxifen-induced AV formation and autophagic cell death via Erk activation.

Although Zn^{2+} accumulation in AVs is a novel finding of the present study, we previously reported that labile Zn^{2+} accumulation occurs in lysosomes of hippocampal neurons under conditions of oxidative stress (Hwang et al. 2008). Our results confirm this hypothesis: control lysosomes were negative for Zn^{2+}, whereas the LC3(+) autolysosomes in cells treated with tamoxifen were loaded with Zn^{2+}. We were unable to determine whether Zn^{2+} accumulation occurs before or after the fusion of AVs with lysosomes because this process occurs very rapidly.

Another issue is the source of Zn^{2+}. Tamoxifen induces oxidative stress in MCF-7 cells, and the antioxidant NAC attenuates the tamoxifen-induced increase in intracellular Zn^{2+}, so it is possible that Zn^{2+} is released from zinc-binding proteins containing

oxidation-sensitive zinc-binding sites, such as metallothionein (MT). MT has 20 cysteines that bind to 7 zinc atoms, and oxidation of these cysteines release 7 zinc atoms (Maret and Vallee 1998). The fact that MT is localized in lysosomes (Klein et al. 1998) suggests MT can be a source of Zn^{2+} in tamoxifen-treated MCF-7 cells. Or it is possible that AVs may have zinc transporters or pumps to take up Zn^{2+}. It is unclear whether vacuolar Zn^{2+} accumulation per se or Zn^{2+} action at upstream cytosolic signaling events is important for autophagy. The development of site-specific zinc chelators would provide the tools necessary to further investigate the mechanism of Zn^{2+} action. Our demonstration that TPEN inhibited tamoxifen-induced increase in the level of LC3-II indicates that Zn^{2+} acts upstream of AV formation. Because TPEN also reduced the level of tamoxifen-induced ROS, it is possible that Zn^{2+} contributes to ROS generation. Further studies are needed to identify the precise site of Zn^{2+} action in autophagy.

Oxidative stress has previously been implicated as an autophagy stimulus (Chen et al. 2008; Scherz-Shouval et al. 2007). It is known that NADPH oxidase plays a role in tamoxifen-indued cell death in hepatoblastoma (Lee et al. 2000b) and that NADPH oxidase inhibitor DPI opposes tamoxifen-induced cell death in MCF-7 cells (Kallio et al. 2005). Consistent with these reports, we found that oxidative stress is a required intermediate event in autophagy; tamoxifen markedly increased the levels of ROS (H_2O_2) in MCF-7 cells, and reducing ROS levels with antioxidants prevented tamoxifen-induced AV formation and Zn^{2+} release. Because tamoxifen-induced MCF-7 cell death is substantially attenuated by antioxidants, an increase in oxidative stress seems to be a prerequisite in the sequence of events leading to cell death. Our results also show that lysosomal enzymes, such as cathepsin D, are released into the cytosol following tamoxifen treatment, and inhibiting cathepsins rescues cells from tamoxifen-induced death. These results demonstrate that LMP may be a key contributor to the mechanism of cell death by tamoxifen-induced overactivation of autophagy. Consistent with the idea that oxidative stress causes LMP via Zn^{2+} accumulation, we found that antioxidants blocked LMP as well as lysosomal and cytosolic Zn^{2+} accumulation.

Under many conditions, autophagy is considered as a physiologic cytoprotective mechanism, since its inhibition causes cell death. However, as shown in the present study, its overactivation also causes LMP and cell death. Hence, for the optimal survival of cells, adequate levels of autophagy may be required. As ROS and Zn^{2+} are linked to autophagy, their cellular levels also should be maintained in certain ranges (Fig. 8). In this regard, it is interesting that tamoxifen-resistant MCF-7 cells exhibit increased levels of cytosolic Zn^{2+} (Taylor et al. 2008). These cells may have altered distribution of cellular Zn^{2+}, and thus may exhibit altered responses to tamoxifen treatment in terms of Zn^{2+} level changes and ROS production.

Our demonstration that labile Zn^{2+} accumulates in AVs and is required for autophagy and cell death in MCF-7 breast cancer cells raises the possibility that dynamic changes in the level of labile Zn^{2+} may have an important role therein. These insights may prove helpful in designing novel therapeutic strategies based on controlling labile Zn^{2+} levels to treat human disease in which aberrant autophagy has been implicated.

References

Bampton ET, Goemans CG, Niranjan D, Mizushima N, Tolkovsky AM (2005) The dynamics of autophagy visualized in live cells: from autophagosome formation to fusion with endo/lysosomes. Autophagy 1:23–36

Bursch W, Ellinger A, Kienzl H, Torok L, Pandey S, Sikorska M, Walker R, Hermann RS (1996) Active cell death induced by the anti-estrogens tamoxifen and ICI 164 384 in human mammary carcinoma cells (MCF-7) in culture: the role of autophagy. Carcinogenesis 17:1595–1607

Chen Y, McMillan-Ward E, Kong J, Israels SJ, Gibson SB (2008) Oxidative stress induces autophagic cell death independent of apoptosis in transformed and cancer cells. Cell Death Differ 15:171–182

Cheng Y, Qiu F, Tashiro S, Onodera S, Ikejima T (2008) ERK and JNK mediate TNFalpha-induced p53 activation in apoptotic and autophagic L929 cell death. Biochem Biophys Res Commun 376:483–488

Choi DW, Koh JY (1998) Zinc and brain injury. Annu Rev Neurosci 21:347–375

de Medina P, Payre B, Boubekeur N, Bertrand-Michel J, Terce F, Silvente-Poirot S, Poirot M (2009) Ligands of the antiestrogen-binding site induce active cell death and autophagy in human breast cancer cells through the

modulation of cholesterol metabolism. Cell Death Differ 16:1372–1384

Ellington AA, Berhow M, Singletary KW (2005) Induction of macroautophagy in human colon cancer cells by soybean B-group triterpenoid saponins. Carcinogenesis 26:159–167

Feng W, Huang S, Wu H, Zhang M (2007) Molecular basis of Bcl-xL's target recognition versatility revealed by the structure of Bcl-xL in complex with the BH3 domain of Beclin-1. J Mol Biol 372:223–235

Frederickson CJ, Koh JY, Bush AI (2005) The neurobiology of zinc in health and disease. Nat Rev Neurosci 6:449–462

Gelmann EP (1997) Tamoxifen for the treatment of malignancies other than breast and endometrial carcinoma. Semin Oncol 24:S1-65–S61-70

Haase H, Maret W (2003) Intracellular zinc fluctuations modulate protein tyrosine phosphatase activity in insulin/insulin-like growth factor-1 signaling. Exp Cell Res 291:289–298

Heerdt AS, Borgen PI (1999) Current status of tamoxifen use: An update for the surgical oncologist. J Surg Oncol 72:42–49

Hwang JJ, Park MH, Choi SY, Koh JY (2005) Activation of the Trk signaling pathway by extracellular zinc. Role of metalloproteinases. J Biol Chem 280:11995–12001

Hwang JJ, Lee SJ, Kim TY, Cho JH, Koh JY (2008) Zinc and 4-hydroxy-2-nonenal mediate lysosomal membrane permeabilization induced by H_2O_2 in cultured hippocampal neurons. J Neurosci 28:3114–3122

Jensen EV, Jordan VC (2003) The estrogen receptor: a model for molecular medicine. Clin Cancer Res 9:1980–1989

Kabeya Y, Mizushima N, Ueno T, Yamamoto A, Kirisako T, Noda T, Kominami E, Ohsumi Y, Yoshimori T (2000) LC3, a mammalian homologue of yeast Apg8p, is localized in autophagosome membranes after processing. EMBO J 19:5720–5728

Kallio A, Zheng A, Dahllund J, Heiskanen KM, Harkonen P (2005) Role of mitochondria in tamoxifen-induced rapid death of MCF-7 breast cancer cells. Apoptosis 10:1395–1410

Klein D, Lichtmannegger J, Heinzmann U, Muller-Hocker J, Michaelsen S, Summer KH (1998) Association of copper to metallothionein in hepatic lysosomes of Long-Evans cinnamon (LEC) rats during the development of hepatitis [see comments]. Eur J Clin Invest 28:302–310

Koh JY, Choi DW (1987) Quantitative determination of glutamate mediated cortical neuronal injury in cell culture by lactate dehydrogenase efflux assay. J Neurosci Methods 20:83–90

Kroemer G, Jaattela M (2005) Lysosomes and autophagy in cell death control. Nat Rev Cancer 5:886–897

Lee TH, Chuang LY, Hung WC (2000a) Induction of p21WAF1 expression via Sp1-binding sites by tamoxifen in estrogen receptor-negative lung cancer cells. Oncogene 19:3766–3773

Lee YS, Kang YS, Lee SH, Kim JA (2000b) Role of NAD(P)H oxidase in the tamoxifen-induced generation of reactive oxygen species and apoptosis in HepG2 human hepatoblastoma cells. Cell Death Differ 7:925–932

Levine B, Kroemer G (2008) Autophagy in the pathogenesis of disease. Cell 132:27–42

Li Y, Maret W (2009) Transient fluctuations of intracellular zinc ions in cell proliferation. Exp Cell Res 315:2463–2470

Liang XH, Jackson S, Seaman M, Brown K, Kempkes B, Hibshoosh H, Levine B (1999) Induction of autophagy and inhibition of tumorigenesis by beclin 1. Nature 402:672–676

Liang XH, Yu J, Brown K, Levine B (2001) Beclin 1 contains a leucine-rich nuclear export signal that is required for its autophagy and tumor suppressor function. Cancer Res 61:3443–3449

Maret W, Vallee BL (1998) Thiolate ligands in metallothionein confer redox activity on zinc clusters. Proc Natl Acad Sci USA 95:3478–3482

Matsui Y, Takagi H, Qu X, Abdellatif M, Sakoda H, Asano T, Levine B, Sadoshima J (2007) Distinct roles of autophagy in the heart during ischemia and reperfusion: roles of AMP-activated protein kinase and Beclin 1 in mediating autophagy. Circ Res 100:914–922

Mizushima N, Levine B, Cuervo AM, Klionsky DJ (2008) Autophagy fights disease through cellular self-digestion. Nature 451:1069–1075

Nixon RA (2006) Autophagy in neurodegenerative disease: friend, foe or turncoat? Trends Neurosci 29:528–535

Park JA, Koh JY (1999) Induction of an immediate early gene egr-1 by zinc through extracellular signal-regulated kinase activation in cortical culture: its role in zinc-induced neuronal death. J Neurochem 73:450–456

Pattingre S, Tassa A, Qu X, Garuti R, Liang XH, Mizushima N, Packer M, Schneider MD, Levine B (2005) Bcl-2 anti-apoptotic proteins inhibit Beclin 1-dependent autophagy. Cell 122:927–939

Plutner H, Davidson HW, Saraste J, Balch WE (1992) Morphological analysis of protein transport from the ER to Golgi membranes in digitonin-permeabilized cells: role of the P58 containing compartment. J Cell Biol 119:1097–1116

Scarlatti F, Bauvy C, Ventruti A, Sala G, Cluzeaud F, Vandewalle A, Ghidoni R, Codogno P (2004) Ceramide-mediated macroautophagy involves inhibition of protein kinase B and up-regulation of beclin 1. J Biol Chem 279:18384–18391

Scherz-Shouval R, Shvets E, Fass E, Shorer H, Gil L, Elazar Z (2007) Reactive oxygen species are essential for autophagy and specifically regulate the activity of Atg4. EMBO J 26:1749–1760

Takeuchi H, Kondo Y, Fujiwara K, Kanzawa T, Aoki H, Mills GB, Kondo S (2005) Synergistic augmentation of rapamycin-induced autophagy in malignant glioma cells by phosphatidylinositol 3-kinase/protein kinase B inhibitors. Cancer Res 65:3336–3346

Taylor KM, Vichova P, Jordan N, Hiscox S, Hendley R, Nicholson RI (2008) ZIP7-mediated intracellular zinc transport contributes to aberrant growth factor signaling in antihormone-resistant breast cancer Cells. Endocrinology 149:4912–4920

Uchiyama Y, Koike M, Shibata M (2008) Autophagic neuron death in neonatal brain ischemia/hypoxia. Autophagy 4:404–408

Vijayanathan V, Thomas TJ, Nair SK, Shirahata A, Gallo MA, Thomas T (2006) Bending of the estrogen response

element by polyamines and estrogen receptors alpha and beta: a fluorescence resonance energy transfer study. Int J Biochem Cell Biol 38:1191–1206

Watts CK, Sweeney KJ, Warlters A, Musgrove EA, Sutherland RL (1994) Antiestrogen regulation of cell cycle progression and cyclin D1 gene expression in MCF-7 human breast cancer cells. Breast Cancer Res Treat 31:95–105

Yamamoto S, Tanaka K, Sakimura R, Okada T, Nakamura T, Li Y, Takasaki M, Nakabeppu Y, Iwamoto Y (2008) Suberoylanilide hydroxamic acid (SAHA) induces apoptosis or autophagy-associated cell death in chondrosarcoma cell lines. Anticancer Res 28:1585–1591

Zheng A, Kallio A, Harkonen P (2007) Tamoxifen-induced rapid death of MCF-7 breast cancer cells is mediated via extracellularly signal-regulated kinase signaling and can be abrogated by estrogen. Endocrinology 148:2764–2777

Zheng X, Chu F, Mirkin BL, Sudha T, Mousa SA, Rebbaa A (2008) Role of the proteolytic hierarchy between cathepsin L, cathepsin D and caspase-3 in regulation of cellular susceptibility to apoptosis and autophagy. Biochim Biophys Acta 1783:2294–2300